

¹³S. Doniach, *J. Chem. Phys.* **70**, 4587 (1979).

¹⁴W. K. Chan and W. W. Webb, unpublished.

¹⁵W. K. Chan and P. S. Pershan, *Phys. Rev. Lett.* **39**, 1368 (1977).

¹⁶W. K. Chan, M. B. Schneider, and W. W. Webb,

in preparation.

¹⁷P. Mueller, private communication, confirmed in our laboratory.

¹⁸J. Doucet *et al.*, *J. Phys. (Paris), Colloq.* **36**, C1-13 (1975).

Fermi-Liquid Droplets in Liquid-Solid Solutions of the Helium Isotopes

B. Hébral, A. S. Greenberg,^(a) M. T. Béal-Monod,^(b) M. Papoular,
G. Frossati, H. Godfrin, and D. Thoulouze

Centre de Recherches sur les Très Basses Températures, Laboratoire associé à l'Université Scientifique et Médicale de Grenoble, Centre National de la Recherche Scientifique, F-38042 Grenoble, France

(Received 31 March 1980)

For temperatures below phase separation of 1000 ppm ³He in solid ⁴He, we measure a heat capacity γT for a pressure between melting of pure ³He and ⁴He. Together with the confined sample geometry, this results in liquid ³He droplets ($\varphi \sim 10^3 \text{ \AA}$) either dilute or pure depending on the phase diagram topology which is discussed theoretically. In the case of a pure ³He droplet, an anomalously high effective mass $m^*/m = 10$ is found, which could be explained by paramagnon effects enhanced by the confined geometry.

PACS numbers: 67.60.-g, 67.50.-b

A possibility for a self-confined geometry, which has been little explored either experimentally or theoretically, is the formation by isotopic separation of a distinct phase of helium in the matrix of the other phase. In this paper we discuss specific-heat results and theoretical considerations of the formation of droplets of liquid helium with typical size 10^3 \AA in a host matrix of solid ⁴He.

The experiment consisted of measuring the heat capacity, C , of a mixture of 1000 ppm ³He from 3 mK to 1 K by applying a heat pulse ΔQ and measuring the corresponding ΔT . The basic apparatus which has been described in detail elsewhere^{1,2} consisted of a cell tightly packed with 22 g of cerium magnesium nitrate (CMN) (filling factor 65%) that served as both refrigerant and thermometer for $T \lesssim 40 \text{ mK}$. From the tight packing of the CMN, we know that the average open volume available to the helium has a diameter between 1 and 5 μm . Our earlier experiments done with the pure liquid and solid phases of both ³He and ⁴He confined in the same cell did not show any anomalous behavior in C_p .² After the last of the pure studies, that of ⁴He, was completed, the cell was evacuated while the apparatus was held at 4 K. To form the isotopic mixtures we condensed $\sim 6 \text{ cm}^3$ STP of pure ³He into the cell and then added pure ⁴He to the extent needed to give pressures

of 90 kPa, 2.2 MPa, and 2.7 MPa. The latter pressure, with an uncertainty of approximately 0.1 MPa, being that of a solid formed with use of the blocked capillary technique starting from liquid at 5.1 MPa and $\sim 2.3 \text{ K}$.³

Our results are displayed in Fig. 1(a) for the two lower pressures in the homogeneous liquid phase. Above 500 mK, C is essentially that of pure liquid ⁴He as we measured earlier,² while for $T < 400 \text{ mK}$ the ⁴He contribution decreases as T^3 and becomes negligible below 100 mK. Below 150 mK and for $T \gg T_F$, the Fermi temperature ($T_F \sim 30 \text{ mK}$ for 1000 ppm⁶), the temperature-independent C is that expected from a noninteracting gas of ³He particles in the classical regime, where the specific heat per atom is $\frac{3}{2}k_B$. This gave us the means, using the low-temperature measured value $C = 3.1 \text{ mJ/K}$, to precisely determine the total number of ³He atoms, 1.5×10^{20} (held constant in this experiment), which will be important in deducing the effective mass discussed later.

The next increase in pressure was planned to bring us between the melting curves of ⁴He, essentially flat at 2.5 MPa below 800 mK, and that of ³He (2.9 MPa at $T \sim 300 \text{ mK}$ to 3.4 MPa at $T = 0$). A similar experiment,⁴ but using a ³He impurity concentration 10 to 20 times larger, showed from NMR measurements that below the isotopic

phase separation temperature the ^3He aggregated into what the authors believed to be droplets of essentially pure liquid ^3He suspended in a matrix of nearly pure hcp ^4He . They estimated a droplet diameter of several microns based on T_1 measurements.

In the present experiment, the size of the droplet was further restricted by the $\sim 1 \mu\text{m}$ CMN cage and smaller concentration of ^3He . This gave a constraint on the maximum size of the droplet $\varphi = x^{1/3}D$, where $D = 1 \mu\text{m}$, $x = 1000 \text{ ppm}$, and thus $\varphi = 1000 \text{ \AA}$ if only one droplet of pure ^3He was formed within the cage. Surface effects can be important since for this droplet size, 5% of the atoms are in the two outer layers.

The results of specific-heat studies presented in Fig. 1(b) show a transition around 150 mK with an associated latent heat, and we believe it marks the phase separation of the solid helium. The temperature agrees well with an extrapolation to small x of the solid helium coexistence curve.⁵ We estimate a latent heat of approximately $5 \mu\text{J}/\text{cm}^3$ by subtracting off a smoothed background heat capacity of $3 \text{ mJ}/\text{K}$. This latent heat is considerably smaller than expected from an entropy of mixing term $\Delta Q = T\Delta S \sim -TRx \ln(x)$ as in Ref. 5. However, it corresponds in order of magnitude to the melting latent heat of the dilute phase which we discuss below.

Below 100 mK, the heat capacity varies linearly with temperature and the proportionality constant $\gamma = 66 \text{ J}/\text{K}^2$ (mole ^3He) corresponds to $C/RT = 8 \text{ K}^{-1}$. It has to be compared to the value 4.85 K^{-1} for pure bulk ^3He at the melting pressure. Translated into effective mass, we get $m^*/m_3 = 10.2 \pm 0.5$ if the droplet is pure ^3He . By comparison the highest value measured in bulk liquid ^3He is $m^*/m_3 = 6.2$ at a pressure 0.7 MPa higher than here.⁶ We show in Fig. 1(b) heat-capacity terms linear in temperature from Ref. 6, and an extrapolation from lower temperatures due to Alvosalo *et al.*⁷ The difference between our measurements and the others is large, and we discuss two interpretations of our results.

Below 100 mK, $C \sim T$ is the signature of a Fermi liquid coexisting with almost pure solid ^4He . The authors of Ref. 4 supposed a pure ^3He liquid phase as indicated by the phase diagrams available in the literature.^{8,9} In fact there may well be a dilute phase which remains stable for a few tenths of MPa above 2.53 MPa (the solidification of pure ^4He), thus giving the proposed phase diagram in Fig. 2.

(i) This topology satisfies continuity require-

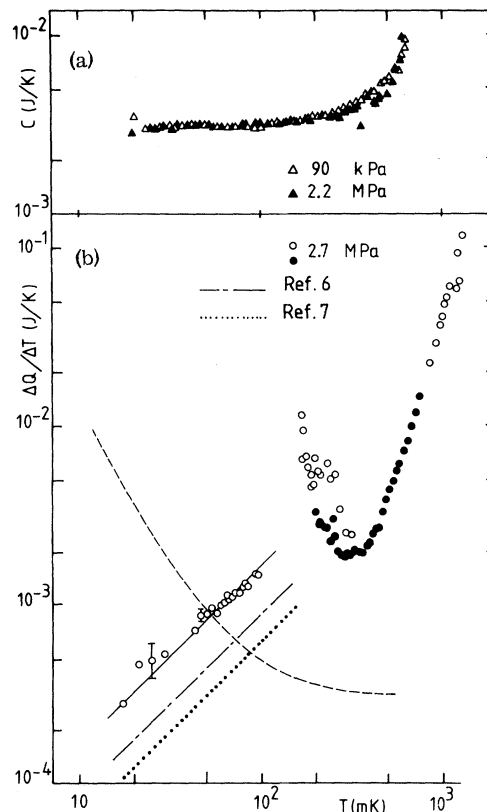


FIG. 1. Heat capacity of 6.2 cm^3 ^4He containing $\sim 1000 \text{ ppm}$ ^3He . (a) Liquid solution, $p = 90 \text{ kPa}$ (open triangles) and $p = 2.2 \text{ MPa}$ (closed triangles). (b) Solid solution, $p = 2.7 \text{ MPa}$. The measurements, taken on warming (open circles) and cooling (closed circles), are displayed as $\Delta Q/\Delta T$ to take into account the latent heat at the transition around 150 mK. The dashed line shows the background heat capacity as measured in Ref. 2. For $T > 60 \text{ mK}$ the experimental uncertainty is about the size of the datum point.

ments, as regards diluted/concentrated liquid ^3He equilibrium, below and above 2.5 MPa. A number of (T, x) diagrams have been systematically investigated at various pressures,^{8,9} but they are hypothetical for $T \lesssim 200 \text{ mK}$. For concentrations below 5% ($< x_0$, the finite solubility of ^3He in ^4He which increases to 10% at 0.8 MPa and slowly decreases to 8% at 2.2 MPa),¹⁰ the behavior seems to be different from all others,⁹ indicating that for the dilute solutions, equilibrium is between phases I and II (Fig. 2) rather than phases I and III.

(ii) The equilibrium condition of phases I and II in Fig. 2 may be written $\mu_3^{\text{II}}(x_c) = \mu_{\text{F}}(x_c) + \mu_3' = \mu_3^{\text{I}} = E_0^s$ (for $T \approx 0$; note that, because of the third law, the phase boundaries are vertical on the $T = 0$ axis). $\mu_3^{\text{II}}(x_c)$ is the chemical potential of ^3He

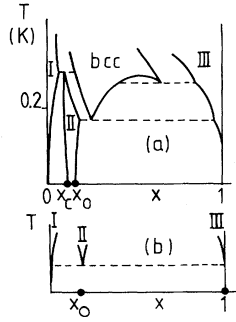


FIG. 2. Proposed phase diagrams (for higher temperatures, see Refs. 8 and 9). I: hcp; II: dilute liquid solution; III: concentrated liquid ^3He . (a) $p < p^*$, (b) $p > p^*$. A triple point (phases I, II, and III) appears at $T = 0$ for $p = p^*$ and rises to finite T for $p > p^*$.

in the dilute liquid phase at minimum solubility x_c . It consists of the perfect Fermi gas potential $\mu_F(x_c) \sim x_c^{2/3}$ plus a correction term¹¹ $\mu_3' = E_0^I - Nx_c|V_0|$, where E_0^I and E_0^S are the rest energies of a ^3He atom in liquid and solid ^4He , respectively. E_0^I is related to L_3 , the latent heat of vaporization per atom of pure ^3He at $T=0$; at saturated vapor pressure $-(E_0^I + L_3) = 0.29 \text{ K}$.¹¹ For zero-point-energetic reasons, we consider the following hierarchy as probable (not too far from ^4He melting pressure): $E_0^I < E_0^S < -L_3 < 0$. We may then extract the *minimum* solubility x_c from a geometrical construction entirely similar to the one that gives x_0 , the maximum solubility.¹¹ x_c is smaller than x_0 , as it should be, as long as $E_0^S < -L_3$. For the pressure p^* where $E_0^S = -L_3$ (i.e., $x_c = x_0$), a triple point, bringing phases I, II, and III into coexistence, would first occur, at $T=0$. We expect p^* to be around 2.8 MPa (see added note). Above p^* , the triple point rises to finite T and equilibrium is between essentially pure solid ^4He and liquid ^3He .

(iii) Coming back to the γT term which has been measured here, we are able to fit this term with an effective mass $m^* \simeq 3m_3$ (which is the relevant figure for dilute solutions at the highest pressures¹⁰), assuming $x_c \sim 8\%$. But to do so, we are forced to consider that only a fraction ~ 0.7 of the total number of ^3He atoms actually contributes to γT . We assume that a single droplet forms in each CMN pore of our restricted geometry with one pseudo-solid monolayer of ^3He atoms at the droplet surface in order to lower its surface tension.¹² For our pore geometry, these absorbed atoms, taken out of the Fermi bath, amount to a large fraction ($\sim \frac{1}{3}$) of the total.

We now examine what happens when the droplets are pure liquid ^3He as in Fig. 2(b) for $p > p^*$. In the following model, we suppose that the droplets are small enough so that the surface to volume ratio, σ , of ^3He atoms is nonnegligible ($10^{-4} < \sigma$ as a rough estimate) and yet large enough for a Fermi-liquid picture to hold, which appears fulfilled in the present experiment. Then each droplet can be regarded as a strongly interacting Fermi liquid in confined geometry. In recent years, it has been shown that, in a nearly magnetic Fermi liquid, the enhanced spin-fluctuations ("paramagnons") already existing in the bulk are expected to be much stronger near the surface.¹³ Then two different types of behaviors can be expected¹⁴ depending on whether \bar{I} , the ratio of the bulk spin-spin interaction in the paramagnon model to the Fermi energy, exceeds or not some critical value \bar{I}_c ($\bar{I}, \bar{I}_c < 1$ and \bar{I}_c depends on the potential exerted by the surface on the single particle wave function of the fermions¹³ in particular the Van der Waals attraction to the surrounding medium¹⁵).

When $\bar{I}_c < \bar{I} < 1$, the central part of the volume remains paramagnetic with the bulk Pauli-type susceptibility constant at very low T , but a few layers next to the surface switch to a two- (or quasi-two-) dimensional itinerant-electron ferromagnetic behavior, with a strong temperature variation of the susceptibility (and the specific heat). This was proposed to apply¹⁵ to liquid ^3He confined in various substrates.¹⁶

But \bar{I}_c is closer to 1 when the ^3He -substrate attraction is weaker,¹⁵ which is the case here with a ^4He substrate in contrast to conventional ones.¹⁶ Then the behavior $\bar{I} < \bar{I}_c < 1$ is more likely to happen. In this case both the central part of the volume and the surface region exhibit Pauli-type susceptibilities, but the surface region is expected to have a larger Stoner enhancement than the central part: The magnitude of the local susceptibility, overenhanced near the surface, decreases from the surface to the center of the droplet, where it would assume the bulk Stoner value at the pressure of the experiment. Therefore, if σ is not negligible, the *overall* effective Stoner enhancement, measuring the ratio of the whole droplet susceptibility to the standard Pauli one of non-interacting fermions, is larger than the bulk one at the same external pressure. Similarly, the overall specific heat still varies linearly with T but with a coefficient much more enhanced compared to the bulk one, yielding anomalously large values of m^*/m_3 . An effective overall interaction

of order ~ 0.98 to 0.99 would give an effective Stoner enhancement of the susceptibility of order 50 to 100 and an m^*/m_3 enhancement of 8 to 11 through $m^*/m_3 = 1 + 4.5\bar{T} \ln[1 + \bar{T}/\{12(1 - \bar{T})\}]$. In that case, interesting associated consequences might be expected: a slight increase of the superfluid ^3He transition temperature,¹⁷ a greater polarizability than in the bulk liquid, etc.

Both situations ($\bar{T} < \bar{T}_c$ and $\bar{T} > \bar{T}_c$) discussed above for liquid He^3 may apply as well to other nearly magnetic metals or compounds in confined geometry (powders or thin films of Pd, for example, could thus exhibit triplet pairing superconductivity or two-dimensional itinerant-electron ferromagnetism¹⁴).

To conclude, we report new experimental and first-stage theoretical investigations of a self-confined phase of liquid helium. According to our proposed phase diagram, one or the other of the above two interpretations will prevail depending on the pressure. Experiments such as neutron scattering and static susceptibility measurements are necessary to obtain more information on the phase diagram, the magnetism, the structure, and the size of the droplets.

Note added.—D. O. Edwards has suggested to us a way of more accurately evaluating the triple point pressure p^* using existing osmotic pressure data. We thus obtain p^* approximately equal to 2.6 MPa. A more detailed discussion will be presented in a paper now in preparation.¹²

We wish to thank E. Varoquaux and P. Leiderer for useful discussions and correspondence. One of us (A.S.G.) acknowledges partial support from the National Science Foundation and the Centre National de la Recherche Scientifique.

^(a)Present address: Service de Physique du Solide et de Résonance Magnétique, Commissariat à l'Énergie Atomique, Orme des Merisiers, BP 2, F-91190 Gif-

sur-Yvette, France.

^(b)Permanent address: Laboratoire de Physique des Solides, Université Paris-Sud, F-91405 Orsay, France.

¹B. Hébral, G. Frossati, H. Godfrin, G. Schumacher, and D. Thoulouze, *Rev. Phys. Appl.* **13**, 533 (1978).

²B. Hébral, G. Frossati, H. Godfrin, D. Thoulouze, and A. S. Greenberg, in *Phonons in Condensed Matter*, edited by H. J. Maris (Plenum, New York, 1980), p. 169; B. Hébral and A. S. Greenberg, to be published.

³E. R. Grilly and R. L. Mills, *Ann. Phys.* **8**, 1 (1959).

⁴A. S. Greenberg, W. C. Thomlinson, and R. C. Richardson, *J. Low Temp. Phys.* **8**, 3 (1972).

⁵D. O. Edwards, A. S. McWilliams, and J. G. Daunt, *Phys. Rev. Lett.* **9**, 195 (1962).

⁶J. Wheatley, in *Progress in Low Temperature Physics*, edited by C. J. Gorter (North-Holland, Amsterdam, 1970), Vol. 6, p. 77.

⁷T. A. Alvesalo, T. Haavasoja, M. T. Manninen, and A. T. Soinne, *Phys. Rev. Lett.* **44**, 1076 (1980).

⁸C. Le Pair, K. W. Taconis, R. De Bruyn Ouboter, P. Das, and E. Dejonc, *Physica (Utrecht)* **31**, 764 (1965); V. L. Vvedenskii, *Pis'ma Zh. Eksp. Teor. Fiz.* **24**, 152 (1976) [*JETP Lett.* **24**, 132 (1976)].

⁹P. M. Tedrow and D. M. Lee, *Phys. Rev.* **181**, 399 (1969).

¹⁰C. Ebner and D. O. Edwards, *Phys. Rep.* **2C**, 77 (1970), and Refs. 47 and 54 therein.

¹¹J. Bardeen, G. Baym, and D. Pines, *Phys. Rev.* **156**, 207 (1966).

¹²B. Hébral *et al.*, to be published.

¹³J. P. Muscat, M. T. Béal-Monod, D. M. Newns, and D. Spanjaard, *Phys. Rev.* **11**, 1437 (1975), and Refs. 4–6 therein.

¹⁴M. T. Béal-Monod and A. Theumann, in Proceedings of the International Conference on Ordering in Two Dimensions, Lake Geneva, Wisconsin, 1980 (to be published); M. T. Béal-Monod, *Solid State Commun.* **32**, 357 (1979).

¹⁵D. Spanjaard, D. L. Mills, and M. T. Béal-Monod, *J. Low Temp. Phys.* **34**, 307 (1979).

¹⁶P. Kumar, *J. Phys. (Paris)*, Colloq. **39**, C6-279 (1978); K. Sato and T. Sugawara, *ibid.*, C6-281; H. M. Bozler *et al.*, *ibid.*, C6-283; A. I. Ahonen *et al.*, *ibid.*, C6-285; H. Godfrin *et al.*, *ibid.*, C6-287; M. T. Béal-Monod and D. L. Mills, *ibid.*, C6-290; D. Spanjaard, D. L. Mills, and M. T. Béal-Monod, *ibid.*, C6-293.

¹⁷K. Levin and O. T. Valls, *Phys. Rev. B* **17**, 191 (1978).